

# The Use of Divertor End Plates as Diagnostics in the Princeton Field Reversed Configuration II

Justin Cohen<sup>1</sup>, Charles Swanson<sup>2</sup> and Samuel Cohen<sup>3</sup>

<sup>1</sup> North Carolina State University

<sup>2</sup> Princeton Satellite Systems

<sup>3</sup> Princeton Plasma Physics Laboratory

E-mail: jtcohen@ncsu.edu

## Abstract

The Princeton Field Reversed Configuration utilizes odd-parity rotating magnetic fields to form and heat an FRC. The reactor includes three main compartments, the Center Cell (CC), Source End Cell (SEC), and Far End Cell (FEC). RMF power is deposited into the Center Cell where it is coupled to a low-density seed plasma that acts as a target. The goal of this experiment was to utilize the divertor plates within the end cells to characterize plasma parameters within those regions of the PFRC-2. It was then possible to use this data to understand particle and energy flow from the center cell. The divertor plate's floating potential, as well as current to ground during RMF discharges were measured to quantify electron energy and density. At an RMF power of 70 kW, a floating potential of -700V was measured on the FEC divertor, which implies electrons with a temperature of 210 eV. An electron density of  $9 \times 10^9$  electrons/cm<sup>3</sup> at 49kW of RMF, was measured in the SEC using the grounded divertor. When the floating potential and current to ground were compared to data from the CC interferometer, there was strong agreement on oscillations seen during electron density decay.

## 1. Introduction

The PFRC is a compact toroid that is currently being developed to burn D-<sup>3</sup>He fuel as a small clean fusion reactor, ideal for spacecraft power and direct propulsion. The potential for spacecraft power up to 10 MW and thrust with high specific power from the one engine would vastly open up the viability of numerous deep space missions, including human missions to Mars. The main mechanism to form and heat the FRC plasma is rotating magnetic fields in an odd parity configuration. The geometry of the device is similar to a mirror machine; however, the induced current creates a very different magnetic topology. The inherent field reversal characterizes the FRC as a high  $\beta$  confinement scheme. The stability of the device is enhanced by passive high temperature superconducting coils that act as magnetic flux conservers. The coils are placed symmetrically about the center line axis and allow for extended pulses of RMF power. To achieve better RMF power absorption, there is an initial steady-state seed plasma produced by a helicon RF antenna which capacitively couples. After this seed plasma is formed, the RMF antenna induce a current in the plasma that opposes the external axial field provided by the coils. In theory, this

induced current is strong enough to fully reverse the field creating a separatrix, which surrounds the region of closed-field lines forming an FRC.

To experimentally validate this process, a suite of diagnostics is used to measure and quantify plasma behavior in the PFRC-2. Most diagnostics including x-ray detectors, fiber optics, diamagnetic loops, and interferometry are non-invasive mechanisms to gather data about the plasma they're studying. In the case of this experiment, the actual divertor end plates which are functionally used to terminate the plasma column, were used to collect data to gain insight on plasma parameters within the regions of the plates, as well as the center cell of the device. There are two configurations which utilize these end plates as diagnostics. One configuration is allowing the end plates to achieve their floating potential during RMF discharges. The floating potentials would change dynamically over the length of the discharge and this data could be recorded by using an HV probe networked to an oscilloscope. The other way the divertor end plates were used as diagnostics was to connect them to ground and measure the current through them during RMF discharges. This was done by surrounding the ground wire with a current measuring device.

Figure 1: PFRC 2 Schematic

Figure 1 shows the overall design of the PFRC (top) along with its axial magnetic field strength along the center line of the device (bottom). The divertor end plates are the Steel cup in the SEC and the moveable brass paddle in the FEC.

## 2. Methodology

One major benefit of the PFRC-2 being a research reactor is, it's highly configurable and has the ability to explore many different operating regimes. There are two different coils that produce the axial field, the L2 coils, and the nozzle coils. The nozzle coils have a small inner radius with the goal of creating a magnetic mirror to reflect incoming gyrating particles. These coils are nominally operated at steady-state at 100A of current. The L2 coils which are the main contributors to the overall magnetic field, are water cooled and can operate up to 430A corresponding to a central field strength of 310G. The fill pressure during pulses is also variable from 0.1mTorr up to 2mTorr. The power delivered by the RMF can currently achieve 70kW of forward power with 25kW of absorbed power.

The divertor end plates which serve to terminate the plasma column are composed of a Tantalum disk of 54mm diameter in the FEC, and a Steel cup of 38mm diameter in the SEC. These surfaces are largely used to protect the surrounding vacuum chamber, and particularly the windows on the chamber in the end cells. The choice to use Tantalum as the FEC divertor plate was due to its low probability of sputtering.

To obtain an equivalent electron energy from a floating potential, some assumptions are necessary. The first is to assume  $T_e > T_i$  which is very accurate for the PFRC-2 as the present RMF frequency is tuned to heat electrons. The next assumption is a Maxwellian temperature distribution. There is validity to this assumption, however previous experiments

have measured a minority population of electrons at a substantially higher energy than the global population. We then assert that the electron current to the probe can be derived as being given by the thermal equilibrium value, being that most electrons are repelled, requiring at least 5% of the bulk population to have enough energy to hit the plate. That would be the random current reduced by the Boltzmann factor:

$$\Gamma_e = \frac{1}{4} n_\infty \bar{v}_e \exp\left(\frac{eV_0}{T_e}\right)$$

The ion current can then be given by the Bohm value, yielding a total electrical current drawn from the probe as:

$$I_{\text{total}} = n_\infty e A_{\text{probe}} \left(\frac{T_e}{m_i}\right)^{1/2} \left[ \frac{1}{2} \left(\frac{2m_i}{\pi m_e}\right)^{1/2} \exp\left(\frac{eV_0}{T_e}\right) - \frac{A_{\text{sheath}}}{A_{\text{probe}}} \exp\left(-\frac{1}{2}\right) \right]$$

Finally, we assume the surface area of the probe to be approximately equal to the area of the sheath around the probe. Then, to solve for floating potential we set the total current equal to zero, as this is the definition of a floating potential. Doing so yields:

$$\frac{eV_f}{T_e} = \frac{1}{2} \left[ \ln\left(2\pi \frac{m_e}{m_i}\right) - 1 \right]$$

This was the direct conversion used to derive an equivalent electron energy from a measured floating potential. To then obtain a density value from the current to ground measurements, it was assumed that there was an equivalent ion saturation current leaving the plasma that was equal in magnitude to the electron current that was measured to ground. The ion saturation current across the sheath surface is:

$$J_i = A_s n_{is} v_{is} = \exp\left(-\frac{1}{2}\right) A_s n_\infty \left(\frac{T_e}{m_i}\right)^{1/2}$$

Thus, by measuring the current to ground and assuming it to be equal to the ion saturation current, knowledge of the geometry of the end plate, and an approximate electron temperature, the electron density can be calculated. Additionally, by performing a Fast Fourier Transform on both the floating potential and current to ground measurements, we can observe what oscillation frequencies are present in those signals.

### 3. Results

To begin to explore the parameter space, the power delivered to the initial seed plasma was varied to observe the dynamics of the floating potential in the divertor regions. The typical seed plasma is extremely tenuous and low energy. The reason for igniting the seed plasma is to make the breakdown time more reproducible. However, it is possible to achieve breakdown with no seed plasma, at higher fill pressures. Under normal operating conditions, the power delivered to the seed plasma antenna is approximately 10W. For this experiment, the seed plasma power was varied from 2.5W to 18W.

#### 3.1 Variable Seed Plasma Power Experiment

The characteristic shape of the Ta paddle floating potential is highly dependent on the operating parameters. When pressure is lower, breakdown is less consistent and can lead to a chaotic signal. Additionally, the more power delivered to the plasma along with a higher axial magnetic field, the more negative the potentials go. The operating parameters for Figure 2 are fairly typical to achieve a stable breakdown.

The floating potentials recorded during the variable seed power experiment were then converted to equivalent electron energies utilizing the procedure outlined in the Methodology.

The highest electron energies for all three landmark voltages, were seen at the highest seed power of 18W as seen on Figure 3. These maximum electron energies were 53.3 eV, 197 eV, and 138 eV for Nominal Seed, Breakdown, and End of Pulse respectively.

#### 3.2 Maximum RMF Power Shot

After observing the correlation with the FEC Ta paddle floating potential and seed power, it was realized that more power input lead to higher energy electrons in this region of the device. Thus, the next step was to observe this relationship with RMF forward power. The proposition of going to higher RMF power is exciting for many reasons, as that would in general lead to more energy deposited into the FRC plasma along with further field reversal. The current power supply utilized to energize the RMF antenna's is limited to delivering higher power due to the risk of melting cables within the circuitry. It was shown that 70.7 kW would be the upper limit to still maintain a stable 4.5 ms duration pulse.

A very interesting behavior was recorded on the FEC disk, as seen in Figure 4. A distinctive staircase like shape over the duration of the pulse, indicated that the energy of electrons hitting the disk were stepping more and more negative. Nearly an identical shape was seen on the Interferometer in the center cell. This shows that as the density decreases in the center cell, this directly correlates to an electron energy gain in the FEC. Additionally, upon analyzing both signals at the location of where the first step down begins at approximately 2.3 ms, both signals start to oscillate. The frequency of these oscillation's is 15 kHz. Thus, the appearance of the same oscillation frequency in both signals, coupled with the same distinct staircase shape, shows a very clear correlation between CC density and FEC electron energy at high RMF power.

Figure 2: Characteristic Floating Potential in the FEC

Nominal Seed

End of Pulse

Operating Parameters	
RMF Pulse Length	6 ms
RMF Power	44 kW
Seed Power	12 w
L2	98 A
Fill Pressure	0.51 mTorr

Breakdown

Figure 2 depicts the shape of the floating potential on the Tantalum disk during the RMF discharge. The negative potential indicates the bombardment of electrons. It is clear that immediately following RMF initiation at time = 0, the highest energy electrons are recorded. Also, there seems to be an oscillation present towards the end of the pulse.

Figure 3: Variable Seed Power Results

Figure 3 shows that all characteristic magnitudes of the floating potential on the Tantalum disk become more negative with increasing power delivered to the seed plasma. The Nominal Seed and End of Pulse values follow the same trend; however, the Breakdown voltage is less effected during lower seed power but does experience a significant drop in voltage at seed plasma > 14W.

Figure 4: Staircase Decay at 70.7 kW RMF Power

## 210 eV Electrons

### 3.3 Grounded SEC End Cup Experiments

The next step in analysing this relationship was to directly compare the density in the center cell as seen by the interferometer, to the density in the end cells. By grounding the SEC divertor end plate and using a current measuring probe encompassing the ground wire, it is then possible to extract electron densities within that end cell region. It must be stated that grounding either end plate of the device is not a passive measurement technique. The large surface area of the divertor plates ( $A_{\text{FEC Plate}} = 92 \text{ cm}^2$ ,  $A_{\text{SEC Plate}} = 45 \text{ cm}^2$ ) is

necessary to effectively terminate the plasma column. These end plates also effectively short circuit magnetic field lines, thus, to allow them to achieve floating potential or connect to ground, can significantly alter the plasma dynamics in those regions of the device. For this experiment however, we were primarily concerned with measuring particle and energy transport from the center cell, therefore, the effects associated with changing the end plate's configuration was not taken into account. However, the decision to ground the SEC plate oppose to the FEC plate was based on the certitude that altering SEC configuration would be less intrusive due to previously observed high energy delivered to the FEC.

Figure 5: SEC Current to Ground

1.2e15 Electrons to  
ground via SEC during  
RMF discharge

3.1e15 Electrons to  
ground via SEC during  
RMF discharge

5.1e15 Electrons to  
ground via SEC during  
RMF discharge

Figure 5 denotes the relationship between current to ground in the SEC and CC density, as the axial field strength increases, shown by the increasing current to the L2 coils. Positive current on the graphs indicate electron current. The total number of electrons leaving to ground was found by integrating the current signal. Additionally, it is possible that a small portion of ions traveled through the nozzle coils and canceled some of the electron current. For these current measurements, it was assumed that the net measured current was proportional to the total electrons in the cell. A clear trend was identified here; as the density in the center cell decreased, the density in the SEC increased, indicative of the direction of particle transport. However, the magnitude of electrons going to ground is a small fraction (1/1000) of total free electrons present in the center cell during the pulse. Additionally, the timing of these events is also identical. The time at which the density begins to decay in the CC is synchronous with the time at which the current to ground rises in the SEC. The point in time during the pulse when these changes in density occurs, appears to be happening earlier in the pulse as L2 increases. Furthermore, the same oscillation (15kHz) is seen on the current to ground measurement as was seen in the FEC floating potential and the interferometer. It is especially clear on the graph for L2 = 124A. Upon performing the analysis discussed in the Methodology to derive electron density from these ground measurements, the following results were obtained:

L2 Current (Amperes)	Electron Density in SEC (Electrons/cm <sup>3</sup> )
92	3.8e9
124	7.5e9
145	9e9

As the L2 current increases and the axial magnetic field strength increased, the electron densities in the vicinity of the SEC end plate also increased, this relationship was fairly linear. It is important to note that these electron densities are 3 orders of magnitude lower than the electron densities in the center cell. The rest of the data from this experiment, including current to ground measurements for higher L2 currents is included in Appendix A.

### 3.4 Oscillation in Floating Potential Analysis

To investigate the floating potential signals on both end plates of the PFRC, a Fast Fourier Transform was performed. The SEC end plate was ungrounded and allowed to achieve its floating potential. Now both divertor's were floating and the FFT was applied. The time domain was split into two regions before applying the FFT. The distinction between the two time domains was the point during the pulse when the signal appeared to oscillate more intensely.

It is clear from Figure 7 that after the transition, both end plates contain the same oscillation, which is also the same frequency seen on the interferometer, 13 kHz. Additionally, the second harmonic of this frequency is present at 26 kHz. The FEC FFT shows how much more stable the FEC is compared to the SEC before the transition point, where the only signal present in the FEC is 470 kHz which is close to the Alfvén Transit Rate. The 15 kHz signal on the SEC could potentially be a precursor to the density decay that occurs at the transition point. The broad peaks present at 120 kHz and 240 kHz could potentially be stable MHD modes.

Figure 6: Floating Potential of Both Divertor Regions

RMF power = 40kW

L2 = 96A

$P_{\text{fill}} = 0.46\text{mTorr}$

It is clear from figure 6 that there is a transition to an instability at  $\approx 4.8\text{ms}$ . The SEC plate reaches more negative potentials compared the FEC plate. However, the SEC floating potential goes closer to zero potential after the transition. It also appears that the SEC floating potential has a higher amplitude oscillation.

Figure 7: FFT of Both End Plates Floating Potentials Before and After Transition

15 kHz

120 kHz

470 kHz

470 kHz

13 kHz

120 kHz

470 kHz

26 kHz

Transition to instability at  $\approx 4.8\text{ms}$

#### 4. Conclusion and Future Work

The divertor end plates of the PFRC-2 were successfully used as diagnostics to measure both floating potential's and current to ground. It was observed that depending on the operating parameters, electron densities are on the order of  $10^9/\text{cm}^3$  with energies between 53 eV and 210 eV. Additionally, it was seen that the density decay in the CC translated to particle and energy flow into the end cells of the device, however the particle gain was 1,000 times less than the total number of particles in the CC. This indicates good confinement within in the FRC core. Future work should aim to apply a sweeping voltage bias to the divertor endplates to obtain more accurate measurements of electron energies and densities.

#### Acknowledgements

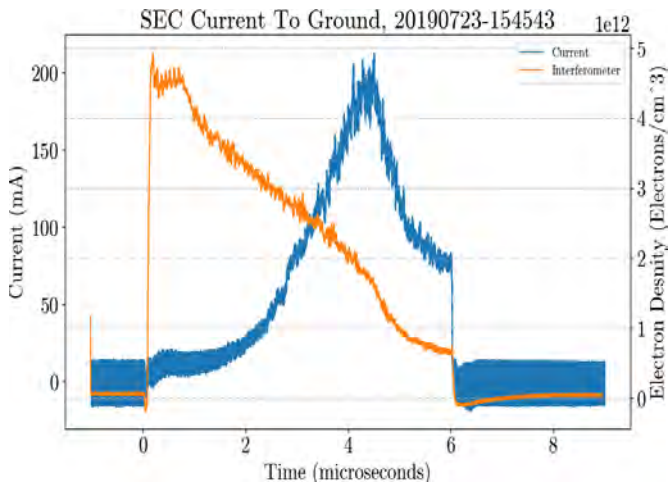
I would like to thank Dr. Sam Cohen and Dr. Charles Swanson for all the support and advice they've given me over the summer. Thanks to Eugene Evans and Eric Palmerduca for explaining all of the intricate details of the PFRC. This work is supported by the US DOE Contract No. DE-AC02-09CH11466.

#### References

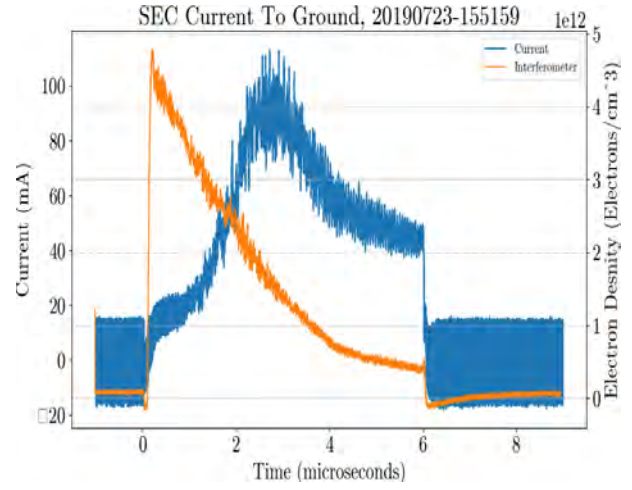
- [1] Cohen, S., et al. "RF Plasma Heating in the PFRC-2 Device: Motivation, Goals and Methods." 28 Dec. 2011, doi:10.1063/1.3664976.
- [2] Hutchinson, Ian H. *Principles of Plasma Diagnostics*. Cambridge University Press, 2005.
- [3] Swanson, C., and S. A. Cohen. "Spontaneous Multi-KeV Electron Generation in a Low-RF-Power Axisymmetric Mirror Machine." *Physics of Plasmas*, vol. 26, no. 6, 2019, p. 060701., doi:10.1063/1.5093905.
- [4] Thomas, Stephanie J., et al. "Nuclear and Future Flight Propulsion - Modeling the Thrust of the DFD"

## Appendix A

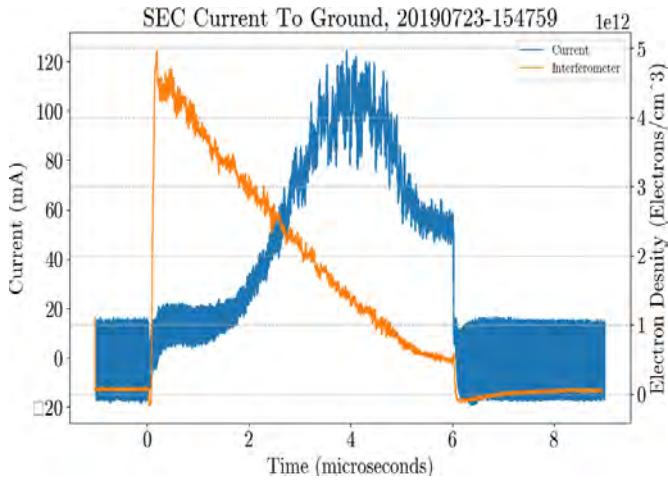
L2 = 165A



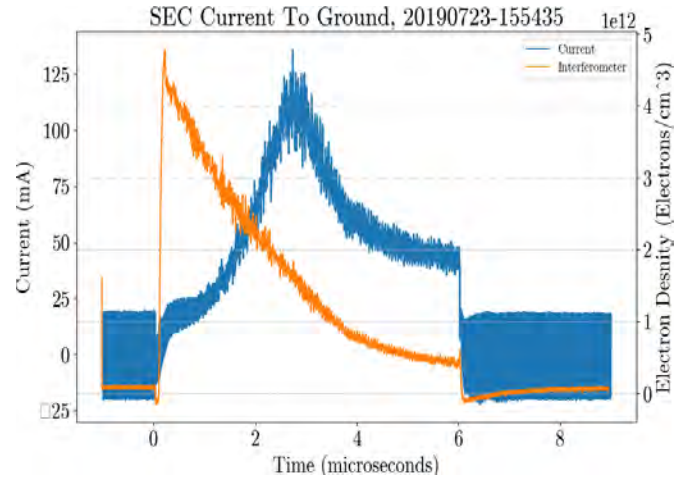
L2 = 231A



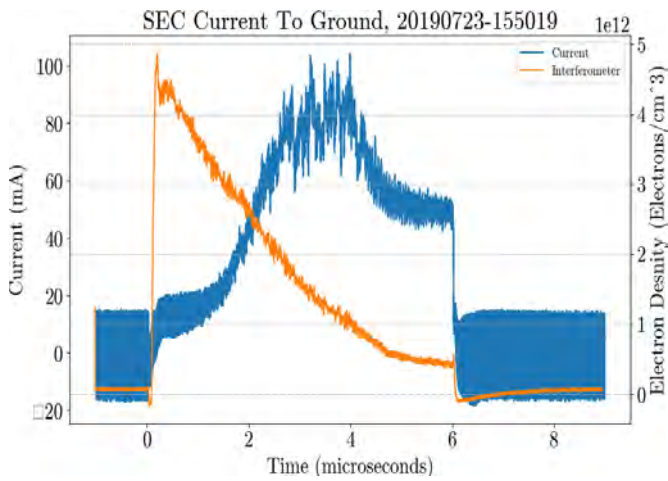
L2 = 186A



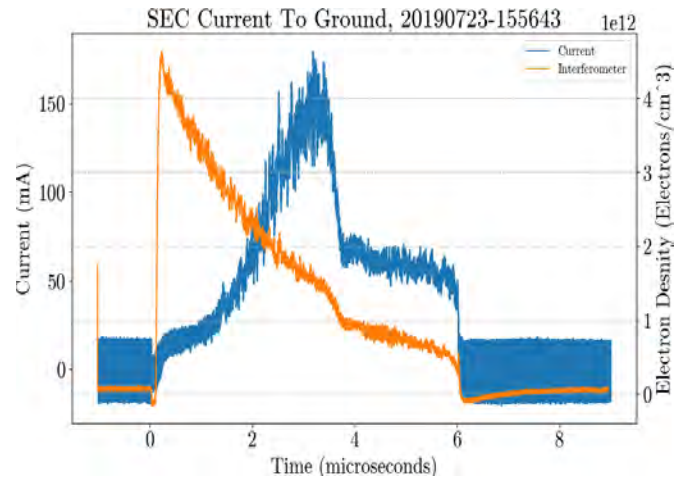
L2 = 247A



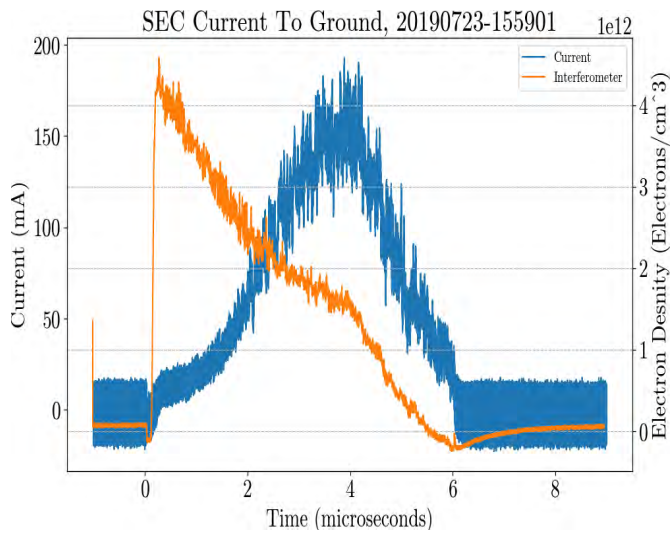
L2 = 207A



L2 = 278A



L2 = 313A



L2 = 346A

